REFERENCES

1. C. Caloz and T. Itoh, Electromagnetic metamaterials: transmission line theory and microwave applications, Wiley-Interscience, Hoboken, NJ, 2006, pp. 1–26.
2. R.A. Shelby, D.R. Smith, and S. Schultz, Experimental verification of a negative index of refraction, Science V 292 (2001), 77–79.
3. J.B. Pendry, Negative refraction makes a perfect lens, Phys Rev Lett 85 (2000), 3966–3969.
4. E.F. Knott, J.F. Shaeffer, and M.T. Tuley, Radar cross section, Artech House, Norwood, MA, 1993.
5. E.F. Kuester, M.A. Mohamed, M. Piket-May, and C.L. Holloway, Averaged transition conditions for electromagnetic fields at a metafilm, IEEE Trans Antennas Propag 51 (2003), 2641–2651.
6. C.L. Holloway, M.A. Mohamed, E.F. Kuester, and A. Dienstfrey, Reflection and transmission properties of a metafilm: With an application to a controllable surface composed of resonant particles, IEEE Trans Electromagn Compat 47 (2005), 853–865.
7. B.A. Munk, Frequency selective surfaces-Theory and design, Wiley, New York, NY, 2000, pp. 14–21.
8. L. Liu, S.M. Matitsine, Y.B. Gan, and K.N. Rozanov, Effective permittivity of lanar composites with randomly or periodically distributed conducting fibers, J Appl Phys 98 (2005), 063512.
9. P.V. Wright, B. Chambers, A. Barnes, K. Lees, and A. Despotakis, Progress in smart microwave materials and structures, Smart Mater Struct 9 (2000), 273
10. O. Reynet, A.L. Adenot, S. Deprot, and O. Acher, Effect of the magnetic properties of the inclusions on the high-frequency dielectric response of diluted composites, Phys Rev B 66 (2002), 094412.
11. D.P. Makhnovskiy and L.V. Panina, Experimental demonstration of tunable scattering spectra at microwave frequencies in composite media containing CoFeCrSiB glass-coated amorphous ferromagnetic wires and comparison with theory, Phys Rev B 74 (2006), 064205.
12. A. Tennant and B. Chambers, A single-layer tuneable microwave absorber using an active FSS, IEEE Microwave Wireless Compon Lett 14 (2004), 46.
13. V. Kisel, Frequency selective or controllable metafilm as a part of on-board antenna screen, Proceeding of Symposium P: Electromagnetic Materials, ICMAT2007, World Scientific Publishing, 2007, pp. 201–208.
14. D.F. Sievenpiper, J.H. Schaffner, H.J. Song, R.Y. Loo, and G. Tangonan, Two-dimensional beam steering using an electrically tunable impedance surface, IEEE Trans Antennas Propag 51 (2003), 2713–2722.
15. D.F. Sievenpiper, J.H. Schaffner, R.Y. Loo, G. Tangonan, S. Ontiveros, and R. Harold, A tunable impedance surface performing as a reconfigurable beam steering reflector, IEEE Trans Antennas Propag 50 (2002).
16. B. Chambers and A. Tennant, Influence of switching-waveform characteristics on the performance of a single-layer-phase switched screen, IEEE Trans Electromagn Compat 44 (2002), 434–441.
17. L. Liu, S. Matitsine, Y.B. Gan, and K.N. Rozanov, The Thickness dependence of resonance frequency in anisotropic composites with long conductive fibers, Electromagnetics 25 (2005), 69–72.
18. L. Liu, S. Matitsine, P.K. Tan, and Y.B. Gan, Smart frequency selective surface with conductive fiber array and diodes, Proceeding of Symposium P: Electromagnetic Materials, ICMAT2007, World Scientific Publishing, 2007, pp. 209–211.

CLUTTER REDUCTION IN SYNTHETIC APERTURE RADAR IMAGES WITH STATISTICAL MODELING: AN APPLICATION TO MSTAR DATA

Sevket Demirci, Caner Ozdemir, Ali Akdagli, and Enes Yigit
Department of Electrical-Electronics Engineering, Mersin University, Ciftlikkoy, Mersin 33343, Turkey; Corresponding author: dr.caner.ozdemir@mersin.edu.tr

Received 30 October 2007

ABSTRACT: *In this article, an application of clutter modeling and reduction techniques to synthetic aperture radar (SAR) images of moving and stationary target acquisition and recognition data is presented. Statistical modeling of the clutter signal within these particular SAR images is demonstrated. Lognormal, Weibull, and K-distribution models are analyzed for the amplitude distribution of high-resolution land clutter data. Higher-order statistics (moments and cumulants) are utilized to estimate the appropriate statistical distribution models for the clutter. Also, Kolmogorov-Smirnov (K-S) goodness-of-fit test is employed to validate the accuracy of the selected models. With the use of the determined clutter model, constant false-alarm rate detection algorithm is applied to the SAR images of several military targets. Resultant SAR images obtained by using the proposed method show that target signatures are reliably differentiated from the clutter background.* © 2008 Wiley Periodicals, Inc. Microwave Opt Technol Lett 50: 1514–1520, 2008; Published online in Wiley InterScience (www.interscience.wiley.com). DOI 10.1002/mop.23413

Key words: *clutter reduction; clutter modeling; synthetic aperture radar; CFAR detection*

1. INTRODUCTION

Automatic target detection and recognition (ATD/R) tools using synthetic aperture radar (SAR) imagery is important in military surveillance applications [1-3]. The aim of an ATD/R algorithm is to identify targets of military significance within SAR images. At the front-end of a typical ATD/R system, target detection is achieved by performing a target hypothesis test for each pixel in the image. During this practice, clutter signal can be really problematic such that target detection becomes a difficult process. Clutter is commonly defined as any unwanted backscattering from the natural environment which interferes with targets and makes target detection a difficult process [4-6]. Hence, clutter has to be reduced to a satisfactorily lower value before ATD/R processing for accurate detection of target signatures.

Most of the clutter reduction techniques incorporate statistical models of the clutter because of the uncertainty of the illuminated area under test [7, 8]. For this reason, numerous papers related to the statistical nature of the clutter have been published in the literature [9-19]. These papers demonstrate the considerably increasing interest in finding the most appropriate statistical distribution to model the clutter. Most commonly adopted models to characterize the clutter statistics are Rayleigh [9], lognormal [10, 11], Weibull [10-14], and K-distribution [15-19]. Yet, determining the best model which describes the land SAR clutter still remains a difficult and challenging task. The main problem arises from inherently complex and statistical behavior of the clutter signal that differs considerably from one application to another. In most practices, the clutter amplitude distribution is governed by various parameters such as the characteristics of random scatterers at the observed surface, range/cross-range resolutions, operating frequency, geometry of illumination (grazing angle), and the data format (power magnitude or signal intensity, single or multilook, etc.) [20]. Therefore, the choice of the best fit for the clutter amplitude distribution should be carried out specifically by means of the empirical application.

In this article, the high-resolution land clutter data of publicly released MSTAR (moving and stationary target acquisition and recognition) SAR images [21] is analyzed for clutter removal and target detection studies. We focused our attention on the three

popular distribution models; namely lognormal, Weibull, and K-distribution. The efficacy of these distributions to model the clutter data derived from MSTAR target images was analyzed, and visual comparisons of the empirical fits of these distributions to the clutter were carried out. Besides, higher-order (HO) statistics such as moments and cumulants were used to determine the best fit to the clutter data. Kolmogorov-Smirnov (K-S) goodness-of-fit test was also applied to quantify the suitability of the selected models. To validate the accuracy of the HO statistics and K-S goodness-of-fit test results, adaptive constant false-alarm rate (CFAR) detector of the selected models was applied to MSTAR target images. Then, the results were compared from the clutter removal and target detection perspective. On the basis of these results, it was shown that successful reduction of clutter is achieved by incorporating the accurate statistical model.

The article is organized as follows: In the next section, commonly used probabilistic models for clutter are reviewed and the non-Rayleigh behavior of the particular clutter amplitude is demonstrated. In Section 3, the experimental clutter data is compared with lognormal, Weibull, and K-distribution models. The best fit to the empirical clutter data is analyzed both graphically and numerically. After concluding the analysis of the clutter data, CFAR detection is applied to target images and the results are discussed at the end of this section. Finally, conclusions and comments on the proposed method are given in the last section.

2. AMPLITUDE DISTRIBUTION MODELS FOR SAR CLUTTER

The first statistical model for the single polarization SAR data was proposed by Goodman [9]. He pointed out that the clutter signal at each pixel in the SAR image could be represented as the superposition of random contributions from many scattering structures inside the radar footprint assuming that the illuminated area was much larger than the wavelength. Hence, the resultant scattered field signal can be represented as [22]:

$$E_s = \sum_{k=1}^{n} M_k e^{j\theta_k} \tag{1}$$

where, n is the number of scatterers, M_k is the amplitude, and θ_k is the phase of the kth component. Assuming the amplitudes are independent random variables and n is sufficiently large; the backscattered field E_s possesses a circular Gaussian distribution as a consequence of the central limit theorem. Then, the amplitude of the backscattered field shows Rayleigh distribution features [9]. The Rayleigh distributed random variable x with parameter σ has a probability density function (PDF) given by

$$p(x) = \frac{x}{\sigma}\exp\left[-\frac{x^2}{2\sigma}\right], x > 0 \tag{2}$$

where x denotes the clutter amplitude. The abovementioned model well matches the clutter amplitude distribution especially for natural radar clutter textures with low resolutions. However, in the case of high-resolution radar and low grazing angles, the clutter distribution deviates significantly from the Rayleigh behavior [10]. For such cases, the models with longer tails than the Rayleigh distribution fit the clutter amplitude better. Therefore, lognormal, Weibull, and K-distributed models are proposed as the alternatives to Rayleigh distributed model. The lognormal PDF [10, 11] has a longer tail than Weibull and K-distribution, and is generally suitable for high-resolution sea clutter and low grazing angles. The PDF of the lognormal distribution is in the form of

$$p(x) = \frac{1}{\sqrt{2\pi}sx}\exp\left(-\frac{1}{2s^2}(\ln x - \mu)^2\right), x > 0 \tag{3}$$

where, μ and s is the mean and standard deviation of the function "ln x," respectively. Another more realistic and useful model is the Weibull distribution [10-14] whose PDF can be characterized by

$$p(x) = bcx^{b-1}\exp(-cx^b), x > 0 \tag{4}$$

where b is the inverse shape parameter and c is the scale parameter. This model has been proven to be a good fit to land clutter especially for low-grazing angles and at high-resolutions [14]. K-distribution is the best suited model for sea clutter and spiky ground clutter [15-19]. The PDF of the K-distribution is given as:

$$p(x) = \frac{2}{a\Gamma(\nu+1)}\left(\frac{x}{2a}\right)^{\nu+1}|K_\nu\left(\frac{x}{a}\right), x > 0, \nu > -1 \tag{5}$$

where a is the scaling parameter, ν is the shape parameter, Γ is the standard gamma function, and K_ν is the modified Bessel function of the second kind of order ν.

3. CLUTTER MODELING AND APPLICATION OF CLUTTER REDUCTION

In this work, we have utilized the publicly released high resolution SAR clutter and target data collected by the MSTAR program [21] for the purpose of clutter modeling and reduction. The MSTAR program is joint Defense Advanced Research Projects Agency (DARPA) and Air Force Research Laboratory (AFRL) effort to develop and evaluate an advanced ATD/R system.

3.1. Parameter Estimation

It is well practiced by the researchers that accurate modeling of clutter involves estimating the parameters of a known probability distribution model that best fits the sample clutter data. In this article, we have analyzed the lognormal, Weibull, and K-distribution in modeling the clutter amplitude of the MSTAR clutter images. The parameters of the lognormal and Weibull distributions were estimated by the well-known maximum likelihood (ML) method which is known as the optimal method for fitting of large samples. By maximizing the log-likelihood function, the ML estimates of the parameters for lognormal distribution can be found as,

$$\hat{\mu} = \frac{1}{n}\sum_{i=1}^{n} ln\, x_i$$

$$\hat{s} = \left(\frac{1}{n}\sum_{i=1}^{n}\ln(x_i - \hat{\mu})^2\right)^{1/2} \tag{6}$$

where, $\{x_i; i = 1...n\}$ are n clutter samples and $\hat{\mu}$ and $\hat{s}$ denotes the mean and standard deviation estimate of "ln x", respectively. In a similar manner, ML estimate of the parameter b of the Weibull distribution (denoted by $\hat{b}$) can be found by solving the equation given below [23]:

$$\left[\sum_{i=1}^{n} x_i^{\hat{b}}\ln x_i\right]\left[\sum_{i=1}^{n} x_i^{\hat{b}}\right]^{-1} - \frac{1}{\hat{b}} - \frac{1}{n}\sum_{i=1}^{n}\ln x_i = 0 \tag{7}$$

Standard iterative techniques such as Newton-Raphson method can be used in solving Eq. (7). Once b is determined; estimate of c (denoted by $\hat{c}$) may then be calculated by:

$$\hat{c} = \frac{n}{\sum_{i=1}^{n} x_i^{\hat{b}}} \tag{8}$$

For the K-distributed model, the ML solution is analytically intractable, so we used HO and fractional sample moments [22] to estimate the parameters in the model. The estimate of the shape parameter ν (denoted by $\hat{\nu}$) is obtained independently from the scale parameter as:

$$\hat{\nu} = \left[\left(\frac{z+2}{2}\right)^2 - \beta_z\right] \Big/ \left[\beta_z - \left(\frac{z+2}{2}\right)\right], \beta_z = \frac{\hat{m}_{z+2}}{\hat{m}_z \hat{m}_2},\ z > 0 \tag{9}$$

In the above equation, z is the parameter that determines the order of fraction and $\hat{m}$ denotes the sample moments given as

$$\hat{m}_r = \frac{1}{n}\sum_{i=1}^{n} x_i^r,\ r \geq 0 \tag{10}$$

where r is the moment order. In this study, we selected the parameter z as 0.5 to reduce the variance of the moment estimates. So, the shape parameter ν is estimated by

$$\hat{\nu} = \left(\frac{25}{16} - \frac{\hat{m}_{5/2}}{\hat{m}_{1/2}\hat{m}_2}\right) \Big/ \left(\frac{\hat{m}_{5/2}}{\hat{m}_{1/2}\hat{m}_2} - \frac{5}{4}\right) \tag{11}$$

provided that $\hat{m}_{5/2}/(\hat{m}_{1/2}\hat{m}_2) \neq 5/4$ as demonstrated in [22]. After determining ν, the estimate of the scale parameter a (denoted by $\hat{a}$) can be obtained by using the moment expression of the K-distribution given below:

$$M_r = \frac{\Gamma(0.5r+1)\Gamma(\nu+1+0.5r)}{\Gamma(\nu+1)}(2\hat{a})^r \tag{12}$$

By replacing the any rth-order moment of this equation with the sample moment one of Eq. (10), the estimated value $\hat{a}$ can directly be solved.

3.2. Modeling the Clutter in MSTAR Images

We began modeling of clutter by first analyzing the statistics of the MSTAR-SAR clutter data observed at a depression angle of 15°. While doing this, we selected one homogeneous and one heterogeneous region of the MSTAR clutter image as shown in Figure 1. The image covers an area of approximately 360 m × 300 m corresponding to a total of 1784 × 1476 data points. Region 1 of this figure contains vegetation texture and it is almost homogeneous. On the other hand, Region 2 consists of forest texture and it is partly heterogeneous. For both regions, we estimated the parameters of the theoretical distributions from the corresponding sample clutter data. During the estimation process, the ML method was used for the lognormal and Weibull distributed models, and HO and fractional sample moments were used for the K-distributed model. Then, we calculated the true PDFs of the distributions with these estimated parameters. Finally, we compared these calculated PDFs with the density histogram of the sample clutter data. The results are presented in Figure 2. The density histogram of the clutter data of Region 1 and the fitted distributions are shown in Figure 2(a). It is seen from this figure that the envelope of the density histogram is in good agreement with Weibull and K-distribution models. In Figure 2(b), corresponding density histogram of Region 2 and fitted distributions are plotted. As easily observed from this figure, the histogram or empirical PDF of this clutter has a tail longer than the previous one. It is also apparent that Weibull and K-distribution can be taken as appropriate models for this particular type of clutter. From these figures, it can be commented that although K-distribution seems to be the best fit, Weibull distribution can also be used in modeling the clutter data in these SAR images.

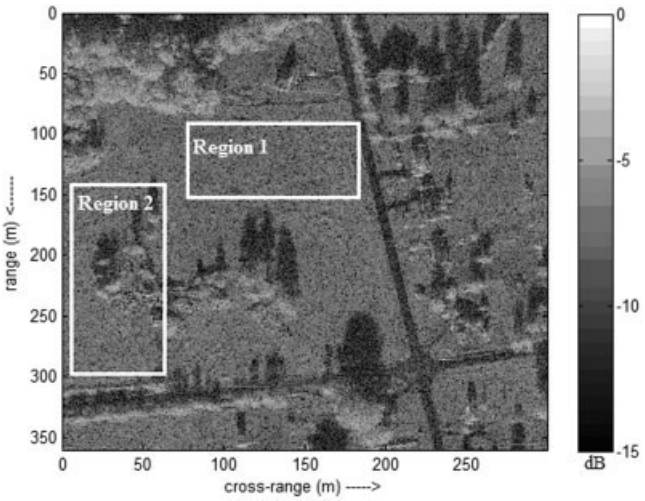

Figure 1 MSTAR SAR clutter image of Huntsville site from Alabama, USA

In this study, our main goal is to reduce the clutter so that we can detect and distinguish the military targets out of these particular SAR images. Therefore, we focused on the MSTAR target images in which various military targets are embedded inside the region of a vegetation clutter. A target free region in the image is selected and the clutter data from this region is analyzed. Using the same clutter analysis procedure emphasized earlier, the density histogram of the clutter data and the calculated PDFs of the theoretical models are plotted in Figure 3(a). As shown in this figure, K-distributed model again fits better than the other two. Also, it is fair that the difference between Weibull and K-distribution is quite small. In addition to this PDF analysis, we also analyzed the empirical cumulative density function (CDF) of the sample clutter data by comparing it with the calculated CDFs of the theoretical distributions. The CDF analysis results are presented in Figure 3(b). It is easy to observe that both Weibull and K-distribution closely follow the empirical CDF of the sample clutter data. This means that, Weibull and K-distribution models can be taken as reasonable models for this clutter data of the target images in any case.

3.3. Comparisons of the Fitting Performance of the Models

Another consideration to assess the underlying model of the clutter data is made by utilizing the moment and cumulant statistics [24] of the both sample clutter data and the model distributions. First, the parameters of the models from the sample data are determined. Then, the HO origin moments, center moments, and cumulants of each model were calculated, and the feature vector of corresponding distribution model based on these data is formed. Afterwards, the vector-based distance of the feature vector of each distribution

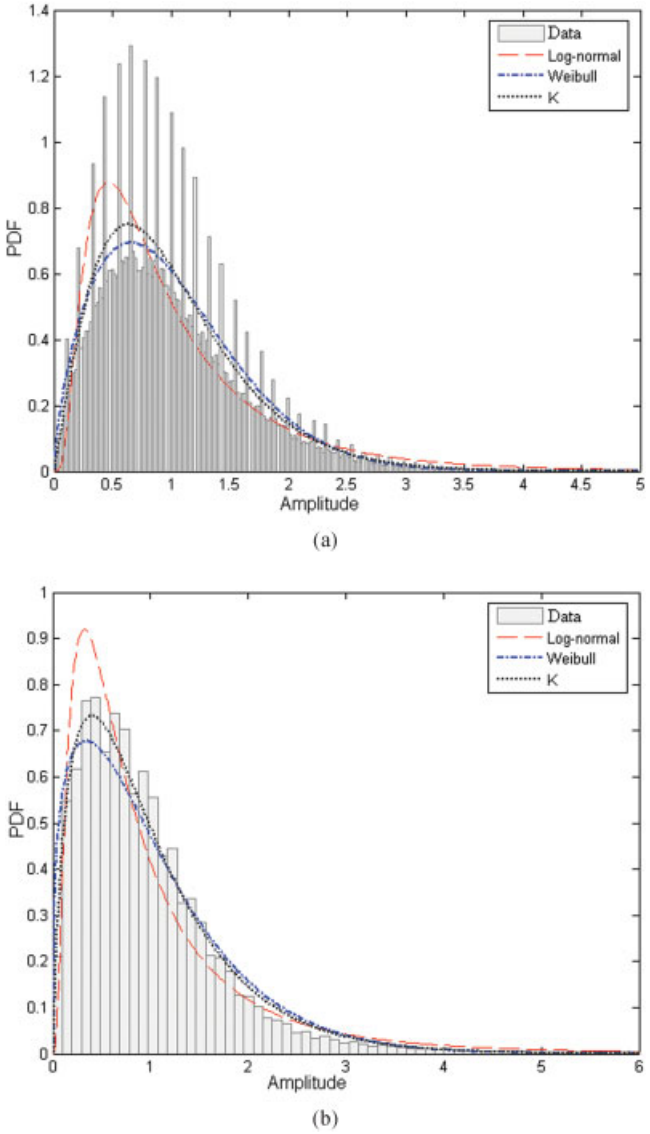

Figure 2 Density histograms and fitted distributions of (a) the vegetation and (b) the forest region of SAR clutter image of Figure 1 (amplitude data is normalized to unity mean). [Color figure can be viewed in the online issue, which is available at www.interscience.wiley.com]

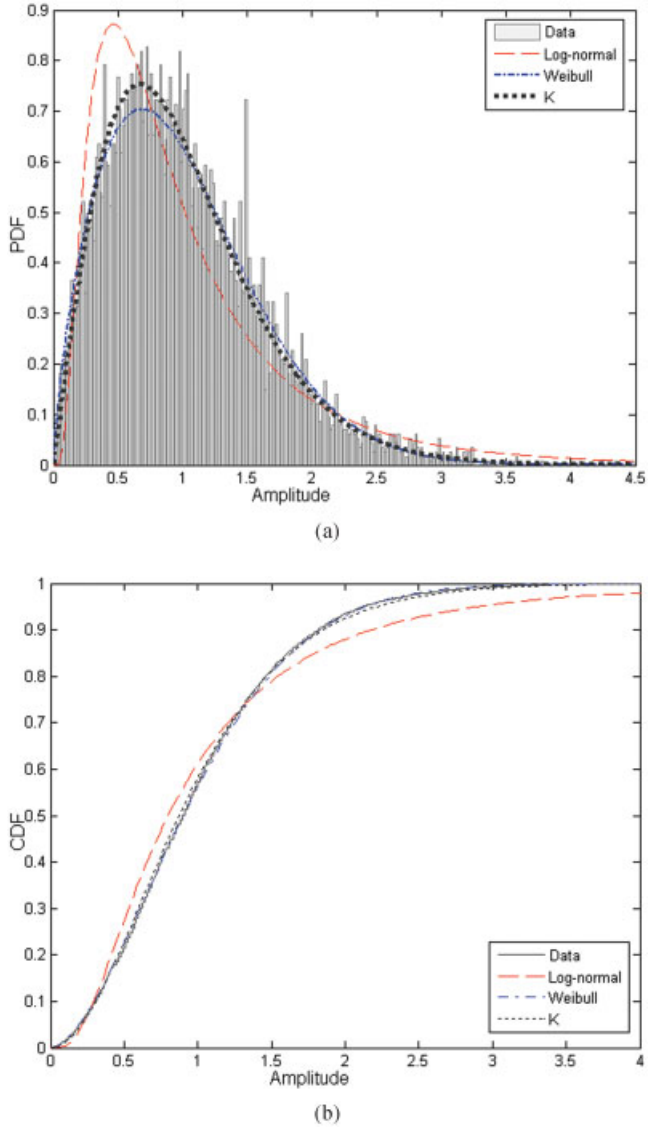

Figure 3 (a) The PDFs and (b) CDFs of clutter data of MSTAR target images and fitted distributions (amplitude data is normalized to unity mean). [Color figure can be viewed in the online issue, which is available at www.interscience.wiley.com]

to the feature vector of sample clutter data was calculated, and the distribution which has a minimum distance was determined. The results of HO statistics for the clutter data of MSTAR target images are given in Table 1. In the calculation of HO statistics, only the first four moments were taken into account. As it is clear from Table 1, K-distributed model has a minimum vector-based distance and can be taken as the best model for the clutter data. Besides, Weibull distributed model has also a small distance and can be used as an alternative model. On the basis of these observations, we can conclude that the numerical results of HO statistics supports the graphical results of the previous section and the clutter data can be modeled with either Weibull or K-distribution.

In addition to the above studies, we also employed the K-S goodness-of-fit test to sample data to check the validity of the Weibull or K-distribution assumption of the clutter model. K-S goodness-of-fit tests use the cumulative distribution function (CDF) approach and therefore belong to the class of "distance tests". In this study, among the several computational methods for the K-S test, the K-S test statistic version [25] was used. In this version, K-S statistic is defined as the maximum value of the absolute difference between the empirical and the theoretical CDFs [25]. To apply this test, we first estimated the parameters of the theoretical distributions (e.g., lognormal, Weibull, and K-distribution) from the sample data. Then, the CDFs of the theoretical distributions were calculated from these estimated parameters and their distance to the empirical CDF of the sample data

TABLE 1
Vector-Based Distance of the Feature Vector (Consists of HO Statistics) of Each Distribution to the Feature Vector of Clutter Sample Data

	Vector-based distance to the feature vector of clutter sample data
Lognormal	77.3499
Weibull	0.6912
K-distribution	0.0221

was evaluated. The results of the K-S test are shown in Table 2 where q is the test value of the K-S test, and τ is the value to compare. The significance level α was selected as 0.05 which means that if $q > \tau$, then the two compared distributions are different with a probability of at least 0.95. As it is demonstrated in Table 2, the calculated test values for the Weibull and K-distribution models are smaller than the compared value. Therefore, they satisfy the distribution of the sample clutter data within the confidence interval of 0.05.

3.4. CFAR Detection and Clutter Reduction

The general procedure to reduce the clutter is the fixed threshold algorithm in which a global threshold is set and applied to the SAR image chip directly [26]. However, this method has the disadvantage that when the target's signal-to-clutter ratio (SCR) is not large enough, most major image features of target are lost while leaving large clutter residues in the image. For an effective clutter reduction, it is necessary to incorporate adaptive threshold algorithms together with the use of an accurate clutter model. CFAR detectors are the most commonly used adaptive threshold routines which ensure the probability of the false alarm to be constant [27]. In a usual CFAR detector, a PDF model for the background data is chosen and the model parameters are estimated by using this background sample data within a sliding window. Then, the probability of false alarm (P_{FA}) for the threshold T is computed by:

$$P_{\mathrm{FA}} = 1 - \int_{-\infty}^{T} p(x)dx = \int_{T}^{\infty} p(x)dx \tag{13}$$

By solving this equation for the threshold T in terms of the specified P_{FA} and the estimated parameters of the PDF $p(x)$, the desired CFAR detector can then be implemented.

Findings of the previous section demonstrated that both Weibull and K-distribution can be chosen as a suitable model for the clutter background. For the implementation of our approach, therefore, the CFAR detectors for only these distributions were investigated in this section. The adaptive threshold value T for the Weibull model can be calculated as:

$$T = \left(\ln\frac{1}{P_{\mathrm{FA}}}\right)^{1/b} a \tag{14}$$

The expression is more complicated for the K-distributed model and T can be calculated by solving the below equation:

$$P_{\mathrm{FA}} = \frac{2}{\Gamma(v+1)}\left(\frac{T}{2a}\right)^{v+1} K_{v+1}\left(\frac{T}{a}\right) \tag{15}$$

Solving this transcendental equation between P_{FA} and T is not trivial. Also, we pointed out in previous sections that the Weibull model fits the clutter data better than the other ones. Hence, Weibull distributed model was selected as the primary in modeling the background clutter. Then, we applied the two-parameter CFAR detector based on this Weibull model [11] which is classified by the rule.

$$x_{\mathrm{t}} \begin{cases} > \mu_b + \sigma_b Q \Rightarrow \text{target pixel} \\ < \mu_b + \sigma_b Q \Rightarrow \text{clutter pixel} \end{cases} \tag{16}$$

where x_{t} is the pixel value under test, Q is a detector design parameter which defines the P_{FA}, μ_b, and σ_b is the estimated mean and standard deviation of the local background, respectively. For each pixel in the image, the corresponding value x_{t} is compared according to the hypothesis test of Eq. (16). If the value of the pixel under test is bigger than the compared value, then it is declared as a target signal. Otherwise, it is classified as clutter and therefore removed from the image.

As the first application, we took the SAR data of military BTR-70 transportation vehicle observed at a depression angle of 15°. The original SAR image is shown in Figure 4(a). The image matrix has a size of 128 × 128 and covers a region of 26 m-by-26 m. The output image of the fixed threshold method is also given in Figure 4(b) for comparison reasons. In the application of the fixed threshold method, the threshold value is determined by trial-and-error method, and any further increment from this value results in increased loss of the target signatures. The result of the CFAR detection for the Weibull modeled clutter background is shown in Figure 4(c). In the implementation of the CFAR detection algorithm, a sliding matrix window of 59 × 59 pixels with a guard area of 19 × 19 pixels was chosen and P_{FA} was set to 0.01. The adaptive threshold value T was calculated from Eq. (14) with the selected probability of false alarm P_{FA}. Then, the design parameter Q was set empirically to $Q = T/\hat{\mu}_{\mathrm{w}}$, where $\hat{\mu}_{\mathrm{w}}$ is the true mean value of the Weibull model with the estimated parameters. If we compare the CFAR output image with the fixed threshold one, the difference is remarkable from both target detection and clutter removal perspective. It is distinguished that target signatures are much more pronounced while the clutter energy inside the image is almost eliminated.

In the second application, we used a target type of BTR-60 transportation vehicle measured at a depression angle of 17°. The original SAR image is shown in Figure 5(a). The corresponding output images of the fixed threshold and CFAR detection method are presented in Figures 5(b) and 5(c), respectively. Same sliding window and guard area settings were used in this example as well. P_{FA} was again selected as 0.01. If we compare the images in Figure 5, it is obvious that the CFAR detection has much better performance than the fixed threshold method. Even though the great amount of clutter is removed from the image, only small amount of target signatures especially resulted from the edges cannot be preserved. Nevertheless, this success of the CFAR detection depends greatly on the accuracy of the selected clutter model.

To sum up, the comprehensive analysis of clutter data of the MSTAR SAR images show that clutter can be well modeled with Weibull distribution. Then, the target signatures can be detected at a high level and clutter can be almost suppressed with this accurate model of the clutter. The success of such detection in turn would help to enhance the accuracy of the further classification and identification stages of ATD/R.

TABLE 2
K-S Test Results of the Distributions with a Significance Level of $\alpha = 0.05$.

	Test value of the K-S test (compared value τ is 0.0642)
Lognormal	0.0719
Weibull	0.0256
K-distribution	0.0182

4. CONCLUSION

In this study, modeling and reduction of undesirable clutter in SAR images were investigated. As a good example of SAR imagery,

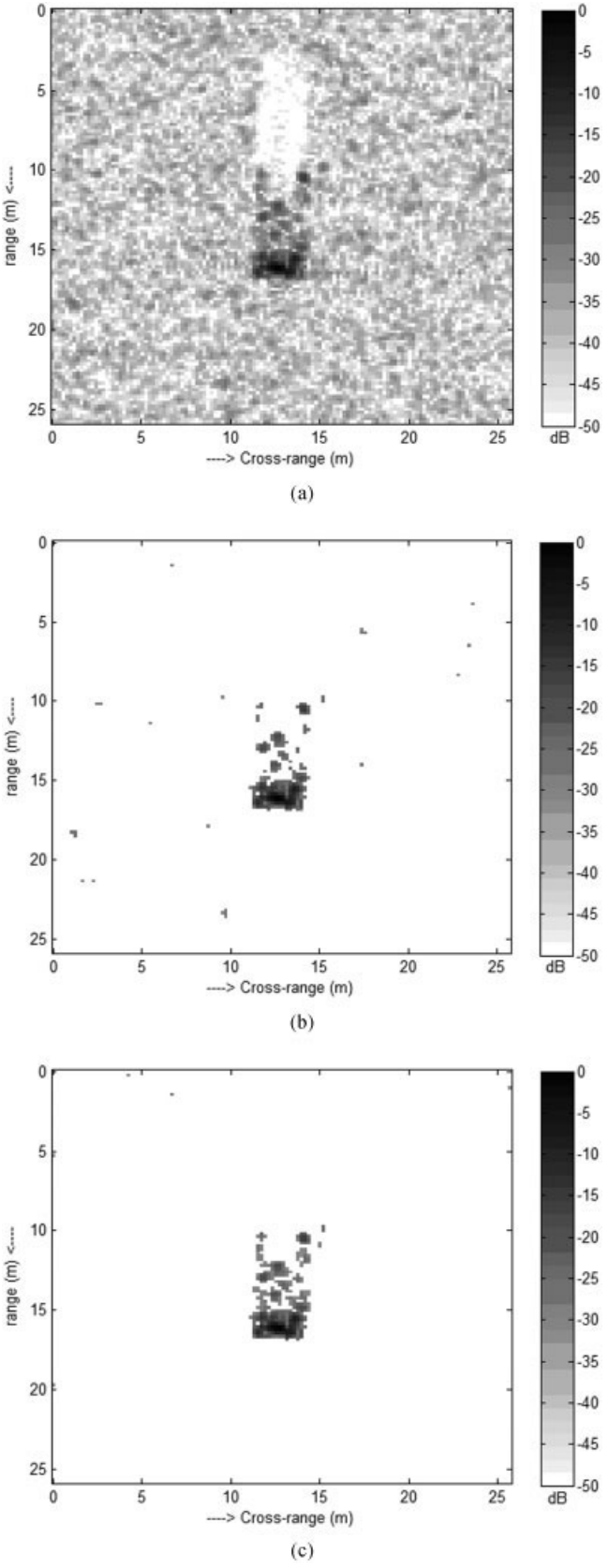

Figure 4 (a) Original SAR image of BTR-70 transportation vehicle with vegetation clutters. (b) Decluttered image with fixed threshold processing. (c) Result of CFAR processing with Weibull clutter assumption and $P_{FA} = 0.01$

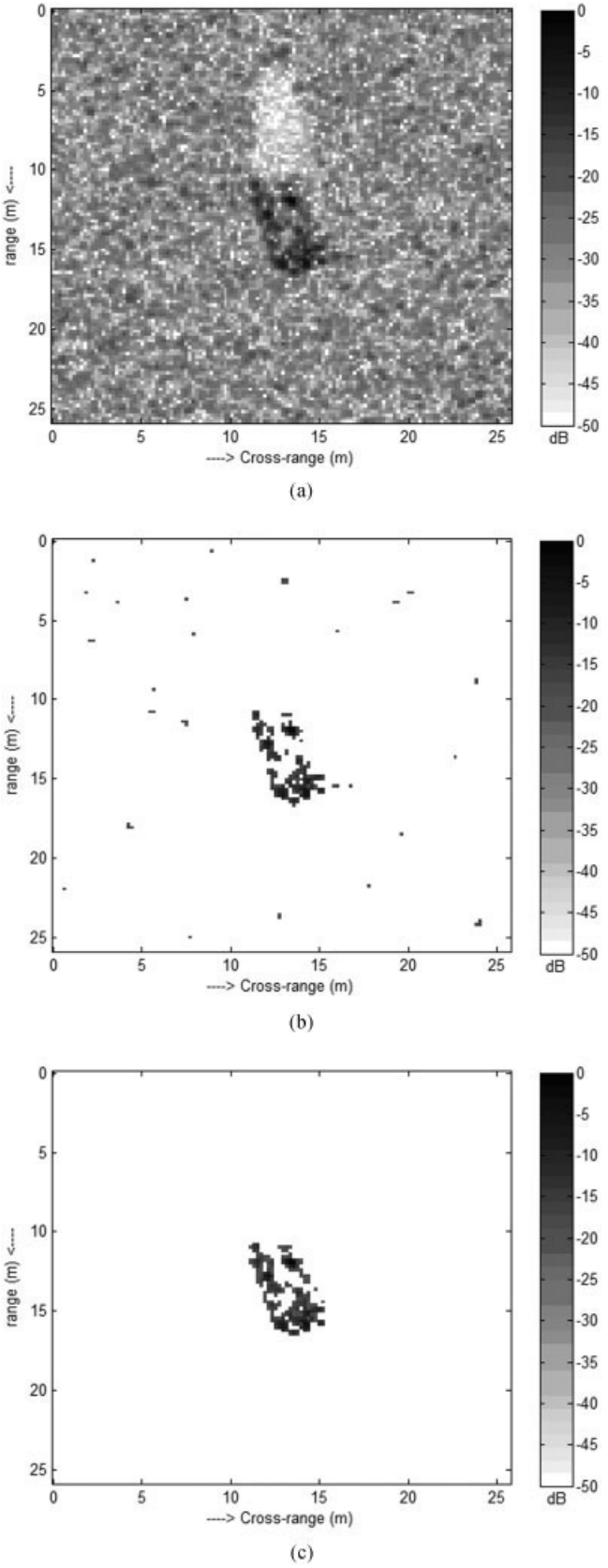

Figure 5 (a) Original SAR image of BTR-60 transportation vehicle with vegetation clutters. (b) Decluttered image with fixed threshold processing. (c) Result of CFAR processing with Weibull clutter assumption and $P_{FA} = 0.01$

publicly released MSTAR images have been selected as the practical application. The statistical and complex nature of clutter was analyzed on this real data of MSTAR clutter chips. Empirical PDF analysis results showed that Weibull and K-distribution models fit closely to the density histograms of both homogeneous and heterogeneous clutter data. Therefore, they can be taken as suitable models for the clutter. Furthermore, the results of HO statistics based on moments and cumulants also supported Weibull and K-distribution model assumptions for the clutter. Finally, the K-S goodness-of-fit test verified the accuracy of these models for the clutter amplitude distribution. Because of the numerical difficulties of K-distribution at the detection stage, CFAR detector under Weibull distributed clutter assumption was selected as the model to use. Then, corresponding CFAR detector based on this model was applied to the target images. Applying the adaptive threshold which was calculated from the PDF of the Weibull distributed model, target signals were effectively segmented from clutter background. Target signature loss was kept at a minimum level and only little false detections were reported. The differences between fixed threshold and CFAR detection algorithm show the notable success of our analysis in modeling the clutter. It should be noted that, although the steps of the modeling and detection algorithm are tested on MSTAR SAR data only, the algorithm can be applied to any SAR image data for clutter removal and reduction purposes.

ACKNOWLEDGMENTS

The authors are grateful to DARPA and Air Force Research Laboratory for providing us MSTAR SAR Clutter and Mixed Targets Data Set. The authors also wish to acknowledge the help and guidance of Dr. Yildirim Bahadirlar at TUBITAK-Marmara Research Center, Gebze, Turkey, who contributed valuable discussions on clutter modeling.

REFERENCES

1. B. Bhanu, D.E. Dudgeon, E.G. Zelnio, A. Rosenfeld, D. Casasent, and I. Reed, Special issue on automatic target detection and recognition, IEEE Trans Image Process 6 (1997).
2. J. Schroeder, Automatic target detection and recognition using synthetic aperture radar imagery, Cooperative Research Center for Sensor Signal and Information Processing, SPRI building, Mawson Lakes Boulevard, Mawson Lakes, South Australia, 2002.
3. M.D. DeVore and J A. O'Sullivan, Performance complexity study of several approaches to automatic target recognition from SAR images, IEEE Trans Aerospace Electron Syst 38 (2002), 632–648.
4. G. Zhang, L. Tsang, and Y. Kuga, Numerical studies of the detection of targets embedded in clutter by using angular correlation function and angular correlation imaging, Microwave Opt Technol Lett 17 (1998), 82–86.
5. J.C. Yoo and Y.S. Kim, A reverse-SAR (R-SAR) algorithm for the detection of targets buried in ground clutter, Microwave Opt Technol Lett 28 (2001), 121–126.
6. D.A. Shnidman, Radar detection in clutter, IEEE Trans Aerospace Electron Syst 41 (2005), 1056–1067.
7. S. Kuttikad and R. Chellappa, Statistical modeling and analysis of high resolution synthetic aperture radar images, Stat Comput 10 (2000), 133–145.
8. C.C. Freitas, A.C. Frery, and A. Correia, The polarimetric G distribution for SAR data analysis, Environmetrics 16 (2005), 13–31.
9. J.W. Goodman, Some fundamental properties of speckle, J Opt Soc Am 66 (1976), 1145–1150.
10. J.B. Billingsley, A. Farina, F. Gini, M.V. Greco, and L. Verrazzani, Statistical analyses of measured radar ground clutter data, IEEE Trans Aerospace Electron Syst 35 (1999), 579–593.
11. G.B. Goldstein, False alarm regulation in Log-normal and Weibull clutter, IEEE Trans Aerospace Electron Syst 9 (1973), 84–92.
12. D.C. Schleher, Radar detection in Weibull clutter, IEEE Trans Aerospace Electron Syst 12 (1976), 736–743.
13. M. Sekine and Y. Mao, Weibull radar clutter, IEE-UK, London, 1990.
14. J.B. Billingsley, Low-angle land clutter measurements and empirical models, William Andrew Publishing, Norwich, NY, 2002.
15. E. Jakeman and P.N. Pusey, A model for non-Rayleigh sea echo, IEEE Trans Antennas Propag 24 (1976), 806–814.
16. C.J. Oliver, Representation of radar sea clutter, IEE Proc F Radar Signal Process 135 (1988), 497–506.
17. S.H. Yueh, J.A. Kong, J.K. Jao, R.T. Shin, and L.M. Novak, K-distribution and polarimetric terrain radar clutter, J Electromagn Waves Appl 3 (1989), 747–768.
18. E. Conte, M. Longo, M. Lops, and S.L. Ullo, Radar detection of signals with unknown parameters in K-distributed clutter, IEE Proc F Radar Signal Process 138 (1991), 131–138.
19. K.D. Ward, R.J.A. Tough, and S. Watts, Sea clutter: Scattering the K distribution and radar performance, Waves Random Complex Media 17 (2007), 233–234.
20. X. Wang, C.-F. Wang, Y.-B. Gan, and L.-W. Li, Electromagnetic scattering from a circular target above or below rough surface, Progress Electromagn Res 40 (2003), 207–227.
21. MSTAR SAR Data Set, Clutter and Targets, Sandia National Lab, released by DARPA, MSTAR Data Collection # 1-2, September, 1995.
22. D.R. Iskander and A.M. Zoubir, Estimation of the parameters of the K-distribution using higher order and fractional moments, IEEE Trans Aerospace Electron Syst 35 (1999), 33–37.
23. C.J. Oliver, Optimum texture estimators for SAR clutter, J Phys D: Appl Phys 26 (1993), 1824–1835.
24. M. Xiaoyan, F. Xueli, Z. Ronghua, and X. Jiabin, An approach of radar clutter recognition based on higher-order statistics combination, In 5th International Conference on Signal Processing Proceedings: WCCC2000, ICSP 2000, Beijing, China, 2000, pp. 1933–1937.
25. N.R. Mann, R.E. Schafer, and N.D. Singpurwalla, Methods for statistical analysis of reliability and life data, Wiley, New York, 1974.
26. D.H. Pham, A. Ezekel, M.T. Campbell, and M.J.T. Smith, A new end-to-end SAR ATR system, In Proceedings of SPIE: Algorithms SAR Imagery VI, Orlando, Florida, 1999, vol. 3721, pp. 292–301.
27. S. Kuttikkad and R. Chellappa, Non-gaussian CFAR techniques for target detection in high resolution SAR images, In Proceedings of IEEE International Conference on Image Process, Austin, TX, 1995, pp. 910–914.